EXPERIMENT NO. 2

INVESTIGATION OF THE STATIC RESPONSE OF A BEAM

Submitted by:

Kush Jani

AEROSPACE AND OCEAN ENGINEERING DEPARTMENT

VIRGINIA POLYTECHNIC INSTITUTE AND STATE UNIVERSITY

BLACKSBURG, VIRGINIA

13 FEBUARY 2025

EXPERIMENT PERFORMED 6 FEBUARY 2025

LAB TEACHING ASSISTANT: KIM HEEJIN

INVESTIGATION OF THE STATIC RESPONSE OF A BEAM

Kush Jani[1]
Virginia Tech, Blacksburg, VA 24060

I. Introduction

The deformation of a structure is crucial to its design criteria and development and theoretical models have thus been created by engineers through history to predict how structures will respond to applied loading conditions. However, validation of these theoretical models is necessary to ensure reliability in the predictions and retain safety for the public that use engineered structures. In this investigation, the static response of a beam is analyzed and compared with predicted theoretical responses to validate the theories and demonstrate the ability of theories while exploring potential sources of uncertainty and error between theory and real-world results. For the investigation, the objectives were:

1. To determine the Young's modulus of the aluminum alloy material of a cantilever beam using static deflection measurements with varied loading at one location.
2. To utilize determined Young's modulus while comparing predicted versus measured deflection for loading at different locations.
3. To tabulate stress and plot against loading utilizing measured strain for varied loading at one location.

These objectives were met through measurements performed in laboratory conditions on a cantilevered beam as shown in Fig 1. This figure depicts the frame which itself contains the beam support, beam, and the resistance strips for the electrical resistance strain gages. Further shown is the P-3500 Strain Indicator and calipers which were used to measure the strain and dimensions of the beam respectively.

As described in brief prior, the goals of the experiment involved analyzing the theoretical models used to predict structure behavior, which involves background knowledge of important concepts for beams such as the Young's Modulus measured and used in the first and second objectives respectively.

The Young's modulus (E), also known as the elastic modulus, is a fundamental material property that defines the relationship between stress and strain in a solid material. The relationship is defined by Hooke's law

$$E = \frac{\sigma}{\epsilon} \tag{1}$$

where E is the Young's Modulus, σ is the stress, and ε is the strain. The Young's Modulus is a material property which should be constant for a given material and is generally measured in Pascals (Pa), representing the ability of a material to resist a deformative loading. The stress of a material represents the internal forces that arise through the application of external forces on a beam and is also generally measured in Pascals (Pa). Strain represents the change in a dimension/length of a beam or material when a force is applied and is a unitless quantity. As a result, the equation defines the exact meaning of the Young's Modulus as being the ratio between the stresses felt by a material and the resulting deformation exhibited by said material.

However, while Eq. 1 will be useful to calculate the stress in order to meet the third objective, the equation will not be useful to calculate the Young's Modulus itself in the current form as stress will be an unknown. However, this brings in the first theoretical model to be analyzed, which is the equation for the deflection of a beam with a single fixed support experiencing an end load:

$$\delta = \frac{FL^3}{3EI} \tag{2}$$

Notably, this formula will be an approximation for the experiments conducted as the beam utilized in the labatory contains two fixed supports (where one support is at the fixed end where the beam meets the frame and the other support is the moveable support 2 inches from the fixed end). Furthermore, the loading applied on the beam will not be at the end of the beam but rather near the end of the beam due to constraints set by the diameter of the weights used requiring the load be applied such that the weights do not collide with the frame towards the free end of the beam. See Fig 2. for an example of such a beam where Eq. 2 would ideally apply. For the purposes of the experiment, the location of the additional support is used as the beginning of the beam and the additional

[1] Undergraduate student, Aerospace & Ocean Engineering Department.

length of the beam past the loading point is unused as the reference deflection somewhat accounts for the additional loading of the beam due to the weight of the material past the loading point. The distributed loading caused by the weight of the beam itself is also unused to allow for simplification in measurements and calculations and due to the unknown density of the beam.

Further background useful for the report is the nature of strain gauges which, as used in this experiment, measure the changes in resistance of the beam caused by strain in the beam. The gauges were bonded to the beam and allowed for the strain to be accurately measured and quantified for the point at which the gauges were located.

The remainder of this report is organized as follows: Section II describes the experimental setup, apparatuses, and techniques used to conduct the experiment while going into more detail on the specific theoreticial models used in calculations. Section III describes the results obtained from the experiment, analyzes the results obtained, and overviews potential points of improvement for further experimentation. Finally, Section IV describes the conclusions and implications gleaned from the experiment while overviewing the insights gained through the procedure and techniques employed throughout the experiment.

II. Apparatus and Techniques

A. Test Structure

The test structure, as shown in Fig 1., consists of a cantilever beam with a rectangular cross-section of an unknown aluminum alloy inside of a frame where one end of the beam is fixed by going through the frame and the other end of the beam is free, as designed by Durelli et al. (1965). The beam's dimensions were determined using a caliper where L represents the length of the longer side of the beam parallel to the lab surface, b represents the length of the shorter side of the beam parallel to the lab surface, and h represents the length of the beam perpendicular to the lab surface (see Fig 3.). Measured dimensions were (L) = 381 mm, (b) = 38.354 mm, and (h) = 6.4008 mm. Note that the length of the beam was calculated using the ruler built into the fixture and was thus converted from inches to milimeters. The vice screw on the frame was tightened towards the fixed end of the beam to prevent the beam from lateral displacement by clamping the beam down on the moveable support and ensure that accuracy was maintained.

B. Loading Mechanism

A loading fixture was tightened onto the beam towards the free end to ensure stability during the first procedure used to meet the first objective (see Fig 4.). As mentioned in the introduction, the loading fixture was not located at the exact free end of the beam but rather a small distance away from the free end due to the inability to have true point loads in reality, necessitating the use of weights with diameters limiting the distance from fixed end the loading fixture could be attached.

The loading fixture itself consists of a mechanism to hang off of the rectangular beam and an eye bolt which could connect to a separate eye bolt that would later be attached to the disk weights. The loading fixture and eye bolt were both weighed and their combined weights (69 grams) were accounted for as part of the point loads on the beam during the measurement phase of the experiment, as shown in Fig 5.

The point loads themselves were disk weights with threaded tapped holes to allow for the use of the eye bolt when hanging on the loading fixture. A combination of five disk weights were used to achieve the desired loading values and were measured and labelled with their masses in grams. The disk weights were 883, 901, 923, 1371, and 1392 grams respectively as shown in Fig 7.

The loading fixture was attached 15 inches or 381 mm from the moveable support, considered the fixed end hereinafter. The point loads on the beam were the disk weights hung on the loading fixture where the force would be the total mass hung times the acceleration of gravity (considered 9.8 m/s^2) as dictated by the equation

$$F = ma \tag{3}$$

where m represents the mass in kilograms and a represents the acceleration due to gravity. In order to meet the second objective, which required the measurement of deflection for various loading locations, the loading fixture was set to three different locations as described in the specifics for said method in Section III.

C. Strain Measurement System

The strain measurement system consists firstly of two connections made by Micro-Measurements Division, Measurements Group, Inc. The connections used for the experiment have a 1.25 inch active gage length with 350 Ohms of resistance and a gage factor of 2.145.

Measurement was accomplished through signals sent by these connections to the Measurements

Group model SB10 Switch and Balance Unit. This unit consists of a Wheatstone bridge circuit in quarter bridge configuration, for which a circuit diagram is shown in Fig 6. The SB10 Switch and Balance Unit takes in the signal from the strain gages and provides an output that can be converted to give the value of the strain experienced by the gages. This is done via the Measurements Group model P-3500 Strain Indicator which provides an output on a digital screen for the microstrain experienced by the gages.

D. Other Equipment

A digital camera was used the photograph the instrumentation, procedures, and set up. A built in ruler atop the frame and a caliper were used to measure dimensions of the various components of the beam system. A Ohaus Scout Pro Portable Electronic Balance was used to measure the mass of each disk weight and loading fixture.

III. Results and Discussion

This section is formatted such that Method 1 describes the procedure and methodology used to meet the first objective, Method 2 describes the procedure used for the second objective, and Method 3 describes the procedure used for the third objective.

A. Method 1: Static Deflection Method for Determining Young's Modulus

In order to determine the Young's Modulus and meet the first objective set out for this investigation, a series of known weights were applied to the cantilever beam and the resulting deflection was subsequently measured using calipers at the location of loading, which remained constant throughout the varying loading conditions. The following formula for deflection caused by loading on a cantilevered beam, as is being approximated for the purposes of this experiment, is used to calculate Young's modulus:

$$\delta = \frac{FL^3}{3EI} \tag{4}$$

This formula is rearranged to solve for E directly using simple algebraic manipulation wherein the equation is divided by δ and multiplied by E, resulting in:

$$E = \frac{FL^3}{3\delta I} \tag{5}$$

In said equation, F represents the applied loading force on the beam, L represents the length of the longer side of the beam parallel to the lab surface, δ represents the deflection of the beam under aforementioned loading, and I represents the moment of inertia (MOI) of the beam, given by equation:

$$I = \frac{bh^3}{12} \tag{6}$$

as b and h (where b represents the length of the shorter side of the beam parallel to the lab surface and h represents the length of the beam perpendicular to the lab surface) are not previously obtained through measurements, they too must be measured alongside the aforementioned F, L, and δ measurements. The MOI of the beam was found to be 838.1701499 mm^4. The remainder of these necessary values were obtained as shown below in Table 1, with the notable assumption that the dimensions L, b, and h of the beam would not change dramatically under the loading conditions selected and were thus only measured rather than for each loading condition. The simplified Eq. 5 is further converted to better account for the location of the loading fixture being further from the free end of the beam than expected by the equation. Manipulation of the equation through integration methods leads to

$$E = \frac{F\mathrm{x}_{loading\ fixture}{}^2((3L)-\mathrm{x}_{loading\ fixture})}{6\delta I} \tag{7}$$

Where $\mathrm{x}_{\text{loading fixture}}$ is the distance of the loading fixture from the fixed end.

Table 1: Static Deflection and Calculated Young's Modulus (Method 1)

Weight (kg)	*Force* (N)	$x_{loading\ fixture}$ (m)	*Deflection δ* (m)	*MOI* (m^4)	*E* (Pa)
0.901	9.506	0.3242	0.0039624	8.38E-10	4105297672
1.371	14.112	0.3242	0.0055118	8.38E-10	4381272598
1.784	18.1594	0.3242	0.006858	8.38E-10	4531157646
2.315	23.3632	0.3242	0.0084074	8.38E-10	4755276499
2.763	27.7536	0.3242	0.009779	8.38E-10	4856574292

The table above has the weights calculated in kilograms. Note that the weights are a combination of the five disk weights outlined in Section II, part A rather than being the five disk weights themselves to provide for greater variance between tested loading conditions. The force was calculated as 9.8 times the mass as outlined in Section II, part B. Note that the table also outlines the unchanging nature of the location of the loading fixture as 324.2 mm or 0.3242 m away from the fixed end of the beam as well as the unchanging nature of the MOI given that the dimensions of the beam were not recalculated per loading condition as aforementioned.

From the measurements, an average Young's Modulus for the beam can be calculated as 45259157419 Pa or 45.2 GPa. While the measurements do show some variation for the Young's Modulus, which should be constant for a material regardless of loading, the variations are minute and the uncertainty calculated was 0.05516326649 GPa (see Appendix, part A). The Young's Modulus physically represents the materials ability to resist deformation and as the value is large, it demonstrates that the aluminum alloy is capable of withstanding large forces with limited deformations.

B. Method 2: Deflection Along the Beam

In order to tabulate the deflection along the beam and compare measured versus predicted values, the loading on the beam was kept the same throughout this part of the experiment. Furthermore, due to the limited variance between deflections at different locations of loading, the largest weight and thus loading force from Method 1 was selected as the standard loading for this method since it would allow for the greatest deflections to be seen, limiting uncertainties, and also allow for greater efficiency in performing Method 2 as one set of data could be copied directly to this method. Therefore, all of the deflections for this method were a result of a 27.7536 N loading condition.

While the loading on the beam was kept the same throughout this method, the location of the hanger itself varied to three different locations along the beam and the measurement of deflection itself was conducted three times per each of these three locations to perform 9 total measurements. To further reduce uncertainty, two trails were conducted for each of the deflection measurements to result in a final total of 18 total measurements being made. The results for these trials is show below in Table 2.

Table 2. Measurement of deflection at different locations along beam due to constant loading

$x_{\delta \text{ for loading } 1}$ (mm)	$\delta_{Trial\ 1}$ (mm)	$\delta_{Trial\ 2}$ (mm)	δ_{Avg} (mm)
177.8	3.0226	3.048	3.0353
279.4	5.8928	8.382	7.1374
381	9.0424	8.9154	8.9789
$x_{\delta \text{ for loading } 2}$ (mm)	$\delta_{Trial\ 1}$ (mm)	$\delta_{Trial\ 2}$ (mm)	δ_{Avg} (mm)
177.8	1.2191	1.143	1.1811
279.4	2.1336	2.0066	2.0701
381	2.667	2.7686	2.7178
$x_{\delta \text{ for loading } 3}$ (mm)	$\delta_{Trial\ 1}$ (mm)	$\delta_{Trial\ 2}$ (mm)	δ_{Avg} (mm)
177.8	2.1336	2.0828	2.1082
279.4	3.9116	3.8354	3.8735
381	5.4864	5.6134	5.5499

The table above references the deflection at loading 1, 2, and 3 which were measured from the free end rather than the fixed end for convenience. The three loading locations were 56.8071 mm, 256.8448 mm, and 151.0284 mm for loading location 1, 2, and 3 respectively. As expected, the deflection was greatest on average for the first loading location followed by the second and third loading locations as the load was furthest from the measuring locations for the first location. This results in a greater deflection as the L in formula

$$\delta = \frac{FL^3}{3EI} \tag{8}$$

is increased and thus the moment arm tha the load is able to act over is significantly greater. The uncertainty (see Appendix, part A) for the results is only 0.024495 mm, which matches the physical behavior expected for the beam.

C. Method 3: Stress Under Static Loading of Beam

Utilizing the same loading conditions and loading location as Method 1, the strain was measured and multiplied with the measured Young's Modulus values from Method 1 in order to calculate stress for plotting as dicated by the rearranging of Hooke's Law (see Eq 1) for stress as follows:

$$\sigma = E\epsilon \tag{9}$$

By measuring the strain values using the strain gauge described prior (see Section II, part C), the creation of a stress vs. loading and strain vs. loading plot can be done to highlight properties of the beam. These strain values are shown in Table 3 below and the subsequently calculated stress values are also shown.

Table 3. Measurement of strain under various loading forces at constant location.

Weight (kg)	*Force* (N)	$x_{loading\ fixture}$ (m)	*E* (Pa)	*Strain* (N/A)	*Stress* (Pa)
0.901	9.506	0.3242	4.11E+10	0.0132	0.59742088
1.371	14.112	0.3242	4.38E+10	0.0207	0.93686456
1.784	18.1594	0.3242	4.53E+10	0.0273	1.235575
2.315	23.3632	0.3242	4.76E+10	0.0358	1.62027784
2.763	27.7536	0.3242	4.86E+10	0.0429	1.94161785

The table above contains the strain results, which are unitless, for the various loading conditions and locations tested. Note that the loading conditions (forces) and locations are the same as those in Method 1 since the strain measurements were collected simultaneously to the deflection measurements to allow for more objectives to be met in the allotted time in the laboratory. As shown by the results, both the strain and stress increase linearly at approximately similar rates which is expected as stress over strain equals the Young's Modulus which is constant. Conceptually, the results also align with physical reality as increased loading would cause greater strain and stress to be experienced by the beam.

IV. Conclusion

The experiment conducted utilized various methods to analyze and validate theoretical models for structural behavior. Measurements made found the dimensions, MOI, deflection, and strain on a beam under various loading conditions and locations to enable the tabulation of the Young's Modulus of the beam and the internal stresses experienced by the beam. The beam was found to have a length of 0.381 m, a base length of 0.038354 m, and a height of 0.0064008 m. This resulted in a calculated MOI of 8.3817E-10 m^4. The investigation involved the use of three procedures. First, the deflections for varying loading conditions at a fixed loading location were collected. Simultaneously, the strain for said conditions and locatiosn were collected. Lastly, the deflection for varying loading locations at a fixed loading condition were collected. The following conclusions were made from the investigation:

1. The beam has a Young's Modulus of 45259157419 Pa or 45.2 GPa.
2. The beam has a linear relationship between stress vs. loading and strain vs loading.
3. The deflection of the beam follows the expected deflection curves for a cantilevered beam undergoing loading at various locations with a non-linear relationship between loading location and deflection.

From the results gathered, comments can be made on the methodology and techniques used throughout the experiments. Firstly, the Young's Modulus does not remain constant as loading is increased and further shows a linear relationship between the increased loading and tabulated Young's Modulus values. From analysis of a least squares trendline used on a Young's Modulus vs. loading condition plot, an R value of 0.9791 is obtained (see Fig 8) which demonstrates a clear and evident linear relationship that should not

exist. However, for the strain vs. load and stress vs. load plots (see Fig 10. And 11. respecitvely), analysis shows an R value of 1 is obtained for both which is validating of the procedures performed as theoretical models confirm the ideal presence of a directly linear relationship between these factors. Finally, for loading at varying locations, the results also confirm the expected result of a non-linear relationship between the location of loading and the subsequent resulting deflection.

The analysis for the Young's Modulus calculation in Method 1 was found to have an uncertainty of 0.05516326649 GPa, while the uncertainty of the deflection calculation in Method 2 was found to have an uncertainty of 0.024494897 mm (see Appendix, part A). While the uncertainty for Method 1 is relatively low, the calculations do not match theoretical models, likely due to simplifcations made throughout the methodology. These simplfications include the lack of accounting for distributed loading caused by the weight of the beam, Poisson's Effect and related changes in dimensions for beams under loading, irregularities in the physical cross-section invalidating the calculation for MOI, and so on. As a result of these simplifications, a possible correlation between loading and Young's Modulus may have been left unaccounted for and resulted in the strong linear relationship found in the tabulation of Young's Modulus against loading. However, the investigation overall met all objectives during the experimentation in the laboratory and mostly validated theoretical models of beams and structures.

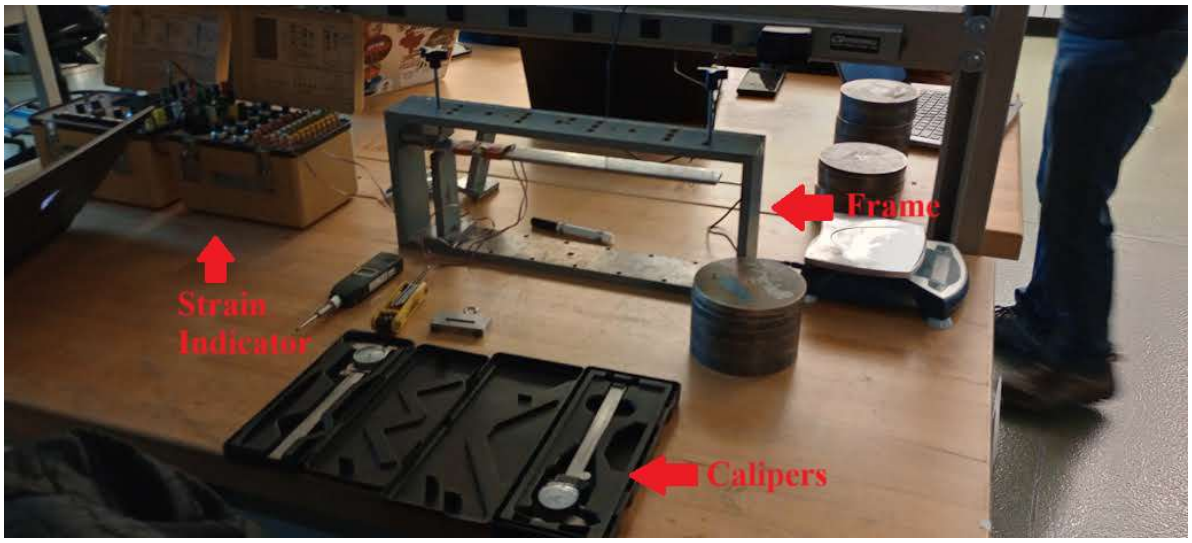

Fig. 1. General Experiment Setup.

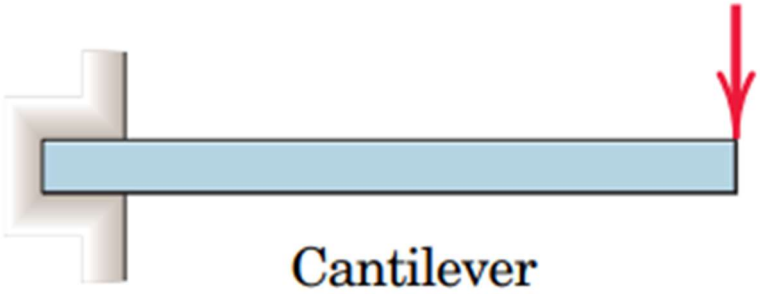

Fig. 2. Example of a Cantilever Beam. From Meriam et al. (2018).

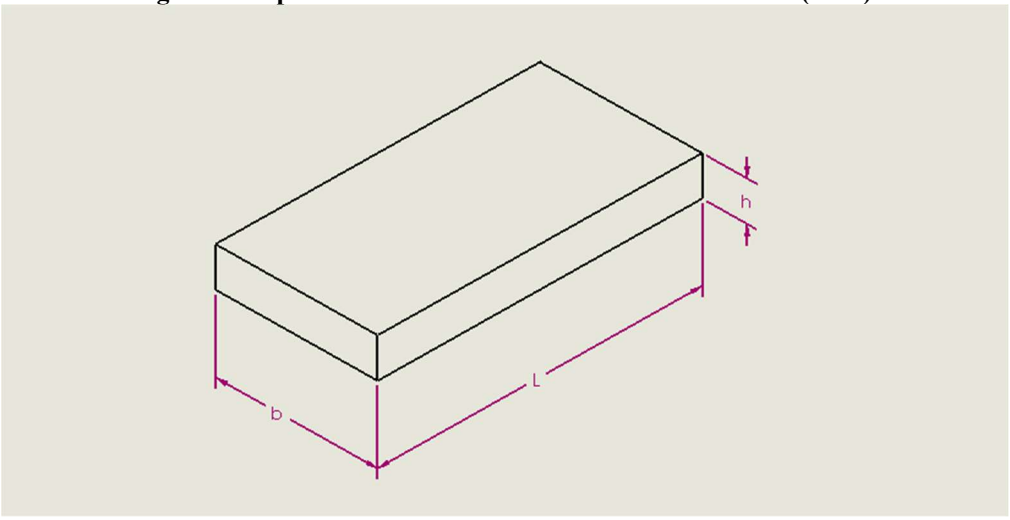

Fig. 3. Dimensions of the Beam from Solidworks Drawing (Not to Scale).

Fig. 4. Tightening of Loading Fixture using Allen Keys.

Fig. 5. Measurement of Loading Fixture and Eye Bolt.

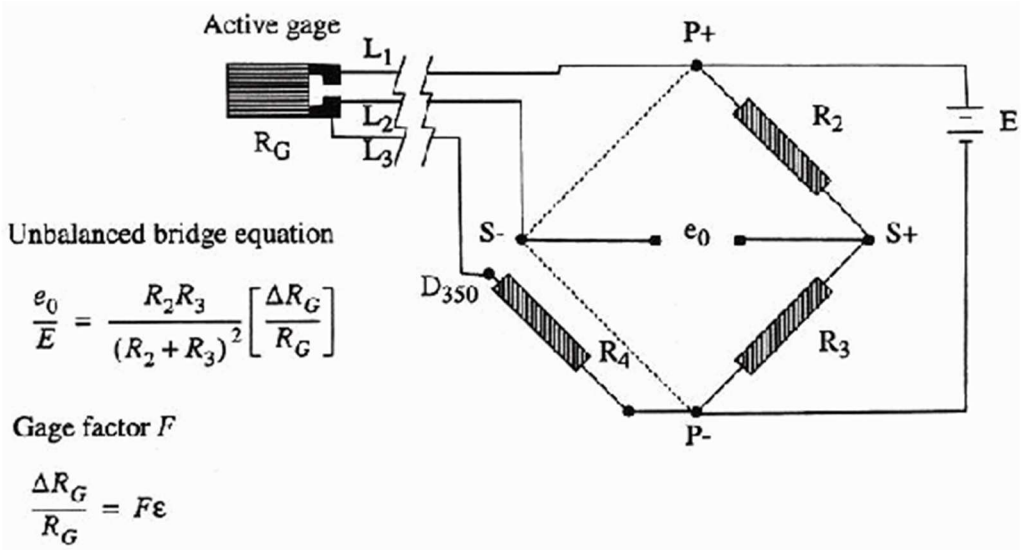

Fig. 6. Quarter-bridge Circuit for Strain Gage Operation. From Hallauer and Devenport (2006).

Fig. 7. Disk Weights Labelled with Respective Masses in Grams.

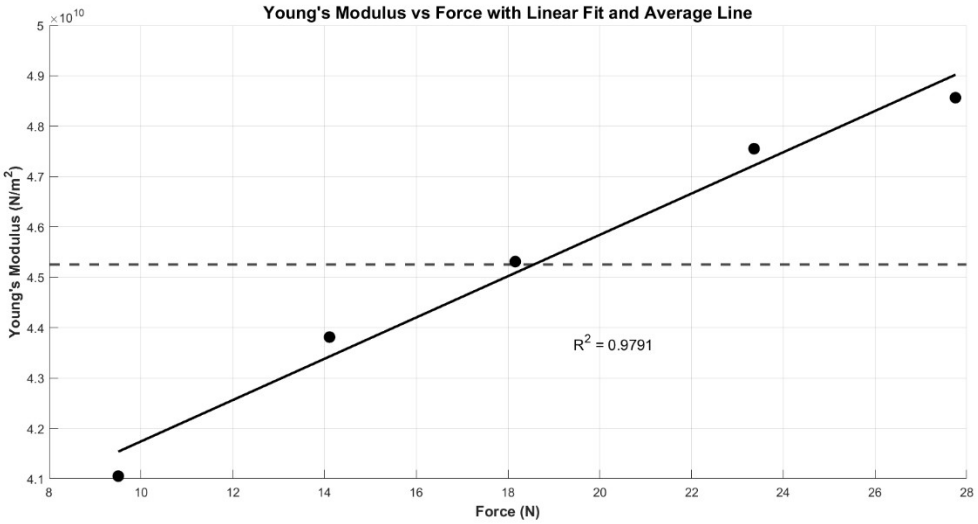

Fig. 8. Young's Modulus (E) vs Weight Force for Method 1 with R^2-Value and $E_{average}$.

```
load = [9.506, 14.112, 18.1594, 23.3632, 27.7536];
E_values = [41052997040, 43812747660, 45311598886, 47552788523, 48565766952];

figure;
scatter(load, E_values, 80, 'MarkerEdgeColor', 'k', 'MarkerFaceColor', 'k');
hold on;

p = polyfit(load, E_values, 1);
f = polyval(p, load);
plot(load, f, 'k-', 'LineWidth', 2);

E_avg = mean(E_values);
yline(E_avg, 'Color', 'k', 'LineWidth', 2, 'LineStyle', '--');

y_mean = mean(E_values);
SS_tot = sum((E_values - y_mean).^2);
SS_res = sum((E_values - f).^2);
R_squared = 1 - (SS_res / SS_tot);

text(max(load)*0.7, max(E_values)*0.9, ['R^2 = ' num2str(R_squared, '%.4f')], 'FontSize', 12, 'Color', 'k');

xlabel('Load (N)', 'FontSize', 12, 'FontWeight', 'bold');
ylabel('Young''s Modulus (N/m^2)', 'FontSize', 12, 'FontWeight', 'bold');
title('Young''s Modulus vs Load with Linear Fit and Average Line', 'FontSize', 14, 'FontWeight', 'bold');

grid on;
hold off;
```

Fig. 9. Code Used to Generate Fig 8.

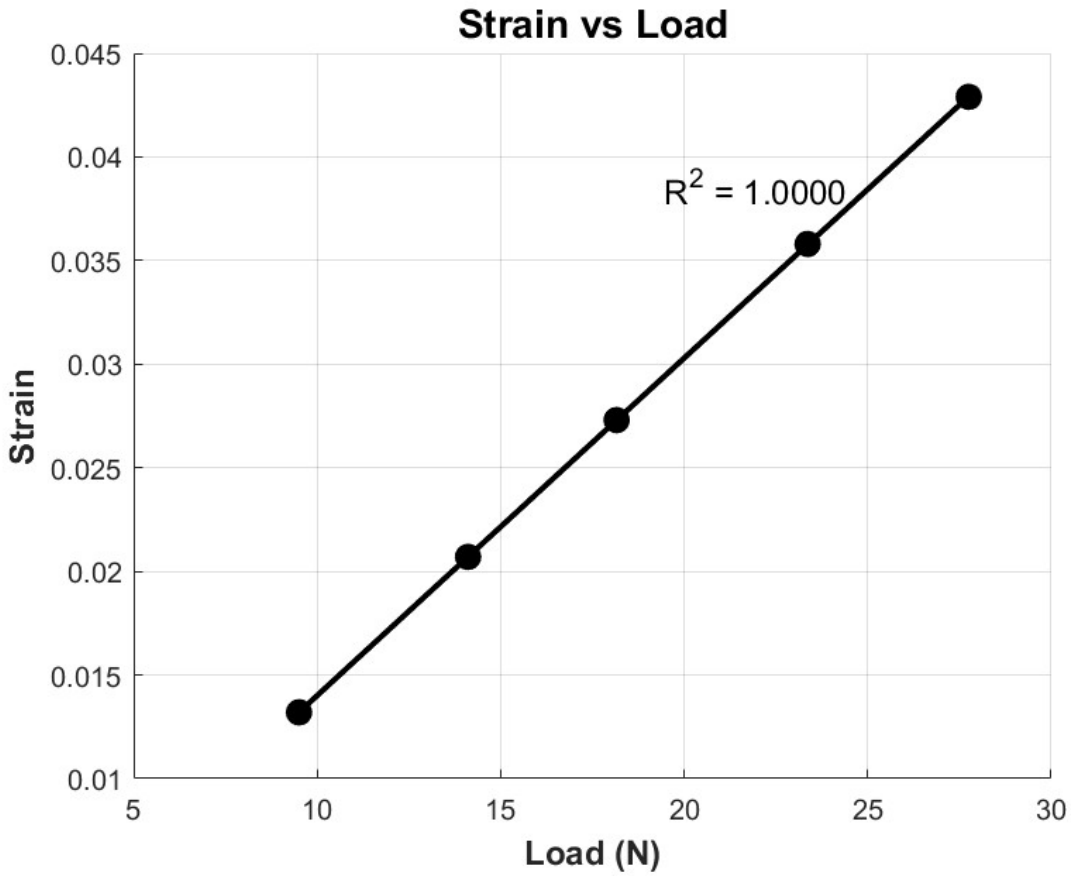

Fig. 10. Plot of Strain vs. Load.

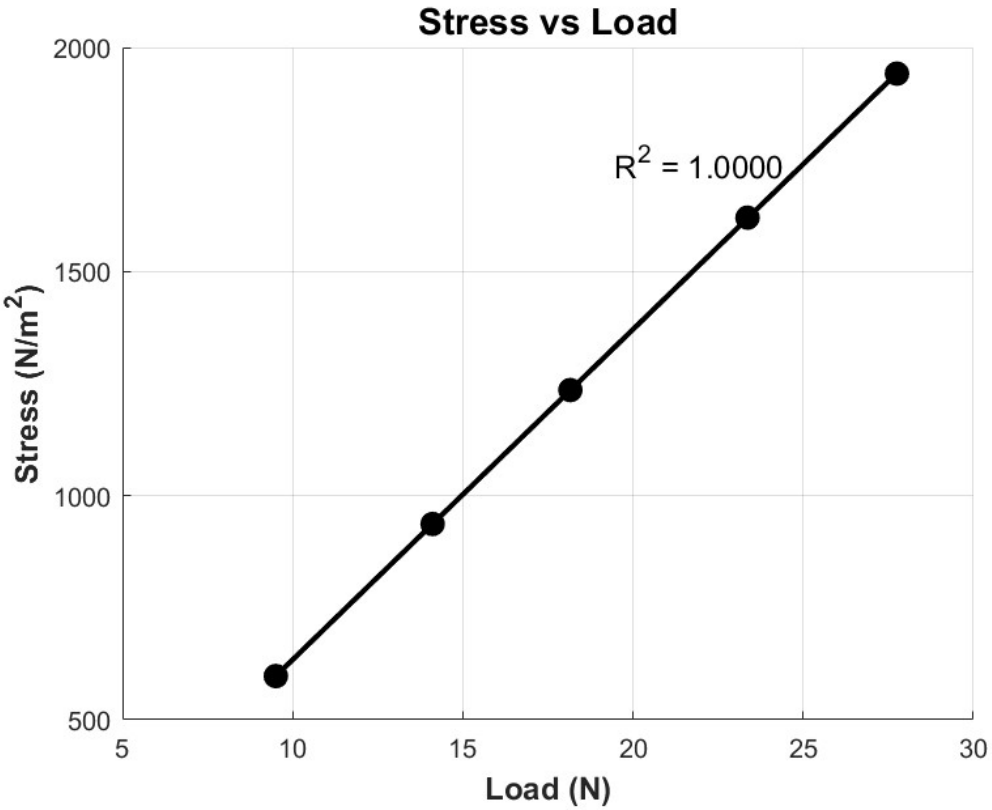

Fig. 11. Plot of Stress vs. Load.

```
load = [9.506, 14.112, 18.1594, 23.3632, 27.7536];
strain = [0.0132, 0.0207, 0.0273, 0.0358, 0.0429];
stress = [597.4208779, 936.8645586, 1235.574998, 1620.277836, 1941.617853];

% Plot 1: Strain vs Load
figure;
scatter(load, strain, 80, 'MarkerEdgeColor', 'k', 'MarkerFaceColor', 'k');
hold on;
p1 = polyfit(load, strain, 1);
f1 = polyval(p1, load);
plot(load, f1, 'k-', 'LineWidth', 2);
R1 = 1 - sum((strain - f1).^2) / sum((strain - mean(strain)).^2);
text(max(load)*0.7, max(strain)*0.9, ['R^2 = ' num2str(R1, '%.4f')], 'FontSize', 12, 'Color', 'k');
xlabel('Load (N)', 'FontSize', 12, 'FontWeight', 'bold');
ylabel('Strain', 'FontSize', 12, 'FontWeight', 'bold');
title('Strain vs Load', 'FontSize', 14, 'FontWeight', 'bold');
grid on;
hold off;

% Plot 2: Stress vs Load
figure;
scatter(load, stress, 80, 'MarkerEdgeColor', 'k', 'MarkerFaceColor', 'k');
hold on;
p2 = polyfit(load, stress, 1);
f2 = polyval(p2, load);
plot(load, f2, 'k-', 'LineWidth', 2);
R2 = 1 - sum((stress - f2).^2) / sum((stress - mean(stress)).^2);
text(max(load)*0.7, max(stress)*0.9, ['R^2 = ' num2str(R2, '%.4f')], 'FontSize', 12, 'Color', 'k');
xlabel('Load (N)', 'FontSize', 12, 'FontWeight', 'bold');
ylabel('Stress (N/m^2)', 'FontSize', 12, 'FontWeight', 'bold');
title('Stress vs Load', 'FontSize', 14, 'FontWeight', 'bold');
grid on;
hold off;
```

Fig. 12. Code Used to Generate Fig 10 and Fig 11.

REFERENCES

Hallauer W. L. Jr. and Devenport W. J., 2006, *AOE 3054 Experimental Methods Course Manual. Experiment 6 - Dynamic Response of a Beam Structure*, A.O.E. Department, Virginia Tech. Blacksburg VA.

Meriam, J. L., Kraige, L. G., & Bolton, D. J., 2018, *Engineering Mechanics: Statics*, 9th edition, Wiley.

Appendix

A. Uncertainty Analysis

In order to perform uncertainty analysis, the primary uncertainties, which involve physical errors in calculations due to equipment limitations, are calculated and combined to get a total uncertainty using the equation

$$\delta(R) = \sqrt{\frac{\partial R}{\partial a}^2 \delta(a)^2 + \frac{\partial R}{\partial b}^2 \delta(b)^2 + \cdots} \quad (10)$$

Shown in Table 4 below is the calculation of uncertainty for the Young's Modulus calculation performed in Method 1. Uncertainties arise for this method through measuring the distance of beam deflection, distance to loading fixture, and width/height measurements. The measurement for the length of the beam is assumed to have no uncertainty and is thus not include in the table. As a result of these primary uncertainties, further derived certainties from the tabulation of the MOI and such other equation-based measurmenets are also calculated and shown.

Table 4. Table for calculation of uncertainty in the Young's Modulus for Method 1.

Variables	*Quantity*	*Primary Uncertainty*	*a+da, b, c, d, e*	*a, b+db, c, d, e*	*a, b, c+dc, d, e*	*a, b, c, d+dd, e*	*a, b, c, d, e+de*	*f+df*	*g+dg*
Beam Length (m)	0.000381	0	0.000381	0.000381	0.000381	0.000381	0.000381	0.000381	0.000381
Distance to hanger (m)	0.000324193	0.00002	0.000344193	0.000324193	0.000324193	0.000324193	0.000324193	0.000324193	0.000324193
Weight Load (kg)	0.901	0.0005	0.901	0.9015	0.901	0.901	0.901	0.901	0.901
Weight (for hanger and hook, kg)	0.069	0.0005	0.069	0.069	0.069	0.069	0.069		0.069
Deflection (m)	3.9624E-06	0.00002	3.9624E-06	3.9624E-06	2.39624E-05	3.9624E-06	3.9624E-06		3.9624E-06
Beam width (m)	0.000038354	0.00002	0.000038354	0.000038354	0.000038354	0.000058354	0.000038354		0.000038354
Beam height (m)	6.4008E-06	0.00002	6.4008E-06	6.4008E-06	6.4008E-06	6.4008E-06	2.64008E-05		6.4008E-06
Intermediate									
Moment of inertia of beam (m^4)	8.3817E-22		8.3817E-22	8.3817E-22	8.3817E-22	1.27524E-21	5.8814E-20		8.3817E-22
Numerator (F*a^2*(3*L-a),	8.18062E-10		8.99588E-10	8.18484E-10	8.18062E-10	8.18062E-10	8.18062E-10		8.18484E-10
Final results									
E (N/m^2 or Pa)	41052976.73		45144181.76	41074138.06	6788481.746	26982655.33	585054.2842		41074138.06
Change			4091205.031	21161.32821	-34264494.98	-14070321.39	-40467922.44		-4070043.703
Uncertainty of E in Pa	55163266.49								

From the tabulations in Table 4, the uncertainty is found to be 55163266.49 Pa or 0.05516326649 GPa.

Shown in Table 5 below is the calculation of uncertainty for the deflection calculation performed in Method 2. Uncertainties arise for this method through measuring the distance of beam deflection when unloaded, loaded for trial 1 and loaded for trial 2. As a result of these primary uncertainties, further derived certainties from the tabulation of the $\Delta\delta_{Trial\ 1}$ and $\Delta\delta_{Trial\ 2}$.

Table 5. Table for calculation of uncertainty in the Young's Modulus for Method 1.

Variables	*Quantity*	*Primary Uncertainty*	*a+da, b, c, d*	*a, b+db, c, d*	*a, b, c+dc, d*
$\delta_{Unloaded}$	51.9176	0.02	51.9376	51.9176	51.9176
$\delta_{Trial\ 1}$ (mm)	54.9402	0.02	54.9402	54.9602	54.9402
$\delta_{Trial\ 2}$ (mm)	54.9656	0.02	54.9656	54.9656	54.9856
Intermediat					
$\Delta\delta_{Trial\ 1}$	3.0226		3.0026	3.0426	3.0226
$\Delta\delta_{Trial\ 2}$	3.048		3.028	3.048	3.068
Final					
$\Delta\delta_{Avg}$ (mm)	3.0353		3.0153	3.0453	3.0453
Change			-0.02	0.01	0.01
Uncertainty of $\Delta\delta$ in mm	0.024494897				

From the tabulations in Table 5, the uncertainty is found to be 0.024494897 mm.